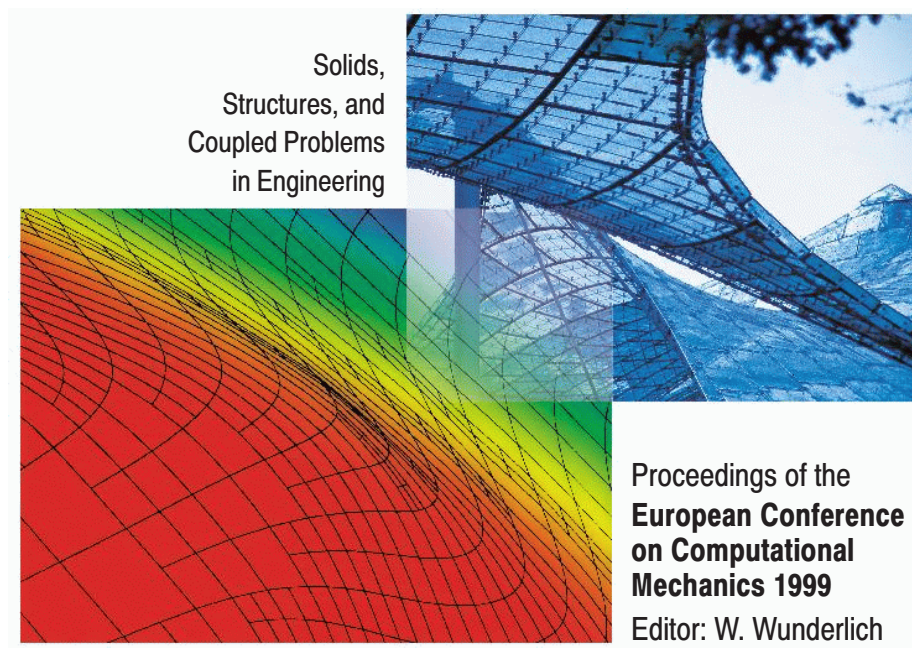


**Dynamics of Shape-Memory-Alloys:  
A Reduction Procedure for 3D Models**

**Melnik, R.V.N., Roberts A.J. and Thomas, K.A.**

**In: Proc. of the European Conference on Computational Mechanics: Solids,  
Structures and Coupled Problems in Engineering,  
W. Wunderlich, Ed.: Munich, Germany, Paper 328, pp. 1--18, 1999**



# ECCM '99

**European Conference on Computational Mechanics**

August 31 – September 3, 1999, Munich, Germany

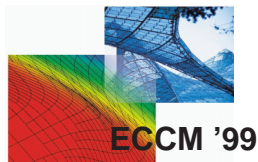
This CD-ROM proceedings contain the papers presented at the first *European Conference on Computational Mechanics* (ECCM '99) held in München (Germany) at the site of the Technische Universität from August 31 to September 3, 1999.

The conference brought together researchers and practitioners from all over Europe and guests from overseas. Its aim was to promote the development of numerical methods in civil, mechanical, naval, aeronautical, and bioengineering, and their application in engineering practice. In particular, it reflects the state-of-the-art of Computational Mechanics in science, software development, and industry. The main focus was directed towards Computational Solid and Structural Mechanics, and Coupled Problems.

The CD-ROM proceedings are printed directly from the electronic versions of the manuscripts provided by the authors. Therefore, the editor can not take responsibility for any inaccuracies, comments or opinions contained in the papers.

Finally, the editor wishes to thank all authors, supporters, and the staff of the local organization for making the ECCM'99 a success. It is my personal wish that this European Conference on Computational Mechanics was the first in a successful series to follow.

*W. Wunderlich*



Munich 1999

## Organization

On behalf of the European Council of Computational Mechanics, the German Association for Computational Mechanics (GACM) was proud to host the first European Conference on Computational Mechanics. It was held in Munich, Germany, at the site of the Technical University, and was organized under the auspices of the International Association for Computational Mechanics (IACM) and the European Community on Computational Methods in Applied Sciences (ECCOMAS).

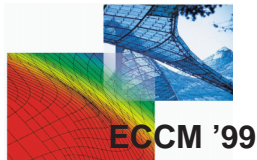
Organizing Committee: **W. Wunderlich**, *München*, Chairman  
**H. Obrecht**, *Dortmund*  
**E. Ramm**, *Stuttgart*  
**E. Stein**, *Hannover*  
**P. Wriggers**, *Darmstadt*

Local Secretariat: **G. Kiener**, *TU München*  
**N. Gebbeken**, *UniBw München*

## Scientific Board of the Conference

The conference was organized with the support of the following IACM/ECCOMAS-affiliated organizations in Europe which are represented in the European Council of Computational Mechanics, ECCM (Chairman: E. Stein). The Scientific Board was formed by their elected delegates:

**J.T. Katsikadelis**, The Greek Association of Computational Mechanics (GRACM), *Greece*  
**M. Kleiber**, The Central European Association for Computational Mechanics (CEACM), *Austria, Czech Republic, Croatia, Hungary, Poland, Slovakia, Slovenia*  
**C. Mota Soares**, The Portuguese Society of Theoretical, Applied and Computational Mechanics, *Portugal*  
**Q. S. Nguyen**, Computational Structural Mechanics Association (CSMA), *France*  
**E. Onate**, Sociedad Espanola de Metodos Numericos en Ingeniera (SEMNI), *Spain*  
**R. Owen**, Association for Computational Mechanics in Engineering (ACME), *United Kingdom*  
**B. Schrefler**, Gruppo Italiano di Meccanica Computazionale (GIMC), *Italy*  
**P. J. Shopov**, The Bulgarian Association of Computational Mechanics (BACM), *Bulgaria*  
**N. E. Wiberg**, The Nordic Association for Computational Mechanics (NoACM), *Denmark, Estonia, Finland, Iceland, Latvia, Lithuania, Norway, Sweden*  
**M. Witkowski**, Polish Association for Computational Mechanics, *Poland*  
**W. Wunderlich**, German Association of Computational Mechanics (GACM), *Germany*  
**P. Z. Bar-Yoseph**, The Israel Association of Computational Methods in Mechanics (IACMM), *Israel*



Munich 1999

## Scientific Advisory Board

**E. R. A. de Oliveira**, *Portugal*

**K.-J. Bathe**, *USA*

**P. G. Bergan**, *Norway*

**R. de Borst**, *The Netherlands*

**E. Dvorkin**, *Argentina*

**M. Geradin**, *Belgium*

**B. Kröplin**, *Germany*

**G. Kuhn**, *Germany*

**P. Ladeveze**, *France*

**O. Mahrenholtz**, *Germany*

**H. A. Mang**, *Austria*

**M. Mikkola**, *Finland*

**J. T. Oden**, *USA*

**J. Orkisz**, *Poland*

**R. Owen**, *UK*

**J. P. Pahl**, *Germany*

**M. Papadrakakis**, *Greece*

**J. Periaux**, *France*

**F.G.Rammerstorfer**, *Austria*

**A. Samuelsson**, *Sweden*

**W. Schiehlen**, *Germany*

**R. L. Taylor**, *USA*

**Z. H. Yao**, *PR China*

**O. C. Zienkiewicz**, *UK*

ECCM '99

European Conference on  
Computational Mechanics

August 31 – September 3  
München, Germany

## DYNAMICS OF SHAPE-MEMORY-ALLOYS: A REDUCTION PROCEDURE FOR 3D MODELS

R.V.N. Melnik

Mathematical Modelling of Industrial Processes,  
CSIRO Mathematical and Information Sciences,  
Locked Bag 17, North Ryde, NSW 1670, Australia  
e-mail: melnik@usq.edu.au

A. J. Roberts, K. A. Thomas

Department of Mathematics and Computing,  
University of Southern Queensland, QLD 4350, Australia  
e-mail: aroberts@usq.edu.au

**Key words:** Shape Memory Alloys, Centre Manifold Technique

---

**Abstract.** *Starting from a general Landau-type 3D model for the shape memory alloy dynamics we have developed a new mathematical “slow manifold” model that allows us to describe effectively the main features of the thermomechanical behaviour of CuAlNi alloys. A robust numerical procedure, developed in our earlier papers for the Falk model, has been generalised to this case. Results of the mathematical modelling of the thermomechanical fields in CuAlNi shape memory alloys are discussed with numerical examples.*

---

- In Section 2 we describe main properties of shape memory alloys that are of industrial importance with the emphasis on copper-based alloys and explain the major difficulties in computational studies of these materials.
- In Section 3 we provide the analysis of different scales used in the modelling of shape memory alloy dynamics.
- Section 4 provides the reader with a three-dimensional Landau-type model used as a core model in our analysis.
- In Section 5 we apply a computer algebra implementation of slow manifold analysis to give a systematic approach for the modelling of thermomechanical behaviour of shape memory alloys on the mesoscopic scale.
- Some computational results obtained with our new model are presented Section 6.
- Conclusion and future directions are discussed in Section 7.

## 2 Copper-based shape memory alloys: thermomechanical properties and difficulties of their computer analysis

Under the action of thermal, mechanical, magnetic, hydrostatic or other fields some materials may restore their original shapes after being deformed. This property is usually termed the shape-memory effect and has been observed in a number of material systems such as metals, ceramics and polymers.

Although a large variety of materials can exhibit the shape memory effect, only those that

- can recover a substantial amount of strain or
- generate significant force upon changing shape

are of current industrial interest. The key in the wide applicability of shape-memory alloys is in a displacive diffusionless process, called the first order martensitic phase transformation, which leads to an internal structural change in the material where in certain temperature regimes two different phases (austenite and martensite) may coexist. We aim for the adequate description of the dynamics of this transformation using tools of mathematical modelling and computational experiment. At present, amongst the shape memory alloy family nickel-titanium (NiTi) and copper-base alloys are the most important. Mechanical properties of these materials vary greatly over the temperature range spanning their transformation. This brings difficulties in determining thermomechanical characteristics of shape memory alloys. For example, if the temperature is slightly above the transformation temperature for this material, we observe a nonlinear pseudoelasticity effect. In this case the material becomes extremely elastic and the elastic characteristics of the material (such as Young's modulus) become strongly dependent on both temperature

and strain deformation. Below we give a brief overview of thermomechanical characteristics of copper-based alloys, in particular copper-aluminium-nickel.

Despite its wide commercial exploitation, NiTi in finished form is very expensive, and in many applications Cu-based alloys such as CuZnAl and CuAlNi provide a more economical alternative to NiTi [29]. Compared to NiTi, a lower recoverable strain of the copper-based shape-memory alloys (around 4% compared to 8.5% for NiTi) has been making these alloys very attractive for the design of different types of actuators.

Perhaps one of the most important advantage of copper-based alloys lies with the fact that they have transformation temperatures well above NiTi alloys. Therefore, where higher temperature actuation is required, CuAlNi alloys are usually preferred since they can give a recovery temperature of up to 190°–200°C (the melting temperature is 1000°–1050°C) [22]. According to Hodgson, Wu and Biermann (see <http://www.sma-inc.com>), with the density 7.12 g/cm<sup>3</sup> commercially available CuAlNi alloys have a thermal conductivity coefficient within 30 – 43 W/(m × °C) and a heat capacity 373–574 J/(kg × °C). These alloys have the yield strength around 400 MPa in the  $\beta$  parent phase and 130 MPa in the martensite (Young's modulus is 85 GPa in the  $\beta$  parent phase and 80 GPa in the martensite), whereas their ultimate tensile strength is up to 500–800 MPa.

Thermomechanical characteristics of CuAlNi have made these shape memory alloys the most appropriate for switching elements in circuit breakers and many other applications [21]. Copper-based shape-memory alloys are becoming more and more important in consumer goods manufacturing and are now used in fire protection devices, in actuators for anti-scald safety valves etc. However, note that these materials are quite sensitive to brittleness (at low temperatures) and instability (they are metastable in nature). The resistivity of these alloys is only 11–13  $\mu\text{Om} \times \text{cm}$  compared to 100  $\mu\text{Om} \times \text{cm}$  in the austenite state (70  $\mu\text{Om} \times \text{cm}$  in the martensite state) for nickel-titanium alloys. This leads to considerable difficulties in modelling the dynamics of CuAlNi alloys undergoing thermally- and mechanically-induced thermoelastic martensitic transformations. Due to its intrinsic metastability, in practical applications this material often requires training (i.e. a progressive modification of the admissible mixtures of martensites and austenite, produced by thermomechanical treatments of the alloy) in order to retain the parent  $\beta$ -phase for shape-memory effects.

Our main results in this paper concern copper-based shape memory alloys, in particular copper-aluminium-nickel alloys.

### 3 Spatial scales for modelling cubic-to-monoclinic phase transformations in copper-based shape memory alloys

The first step in the construction of mathematical and computational models for the analysis of thermomechanical behaviour of shape memory alloys is the choice of an appropriate spatial length scale. In principal, such models can be constructed on any of the atomic-, meso- or macro-scale levels. However, the deformation process of the phase transformation

simulated on the computer will be strongly dependent on the length of observation. In the majority of current applications the required length of observation may vary from a few nanometers to hundreds of micrometers ( $\approx 10^{-9}$ – $10^{-4}$  m).

Using the Landau-Devonshire phenomenology, established by Falk on the mesoscopic scale, in our earlier papers [14, 15] we performed a computational analysis of the austenitic-martensitic phase transitions of shape memory alloys described by the following model

$$\begin{cases} C_v \left[ \frac{\partial \theta}{\partial t} + \tau_0 \frac{\partial^2 \theta}{\partial t^2} \right] - k_1 \left[ \theta \frac{\partial u}{\partial x} \frac{\partial^2 u}{\partial t \partial x} + \tau_0 \frac{\partial}{\partial t} \left( \theta \frac{\partial u}{\partial x} \frac{\partial^2 u}{\partial t \partial x} \right) \right] - \mu \left[ \left( \frac{\partial^2 u}{\partial t \partial x} \right)^2 + \right. \\ \left. \tau_0 \frac{\partial}{\partial t} \left( \frac{\partial^2 u}{\partial t \partial x} \right)^2 \right] - \nu \left[ \frac{\partial \theta}{\partial t} \frac{\partial^2 u}{\partial t \partial x} + \tau_0 \frac{\partial}{\partial t} \left( \frac{\partial \theta}{\partial t} \frac{\partial^2 u}{\partial t \partial x} \right) \right] - \frac{\partial}{\partial x} \left( k \frac{\partial \theta}{\partial x} \right) = G, \\ \rho \frac{\partial^2 u}{\partial t^2} - \frac{\partial}{\partial x} \left[ k_1 \frac{\partial u}{\partial x} (\theta - \theta_1) - k_2 \left( \frac{\partial u}{\partial x} \right)^3 + k_3 \left( \frac{\partial u}{\partial x} \right)^5 \right] - \mu \frac{\partial^3 u}{\partial x^2 \partial t} - \nu \frac{\partial^2 \theta}{\partial x \partial t} = F, \end{cases} \quad (1)$$

where  $u$  is the displacement field,  $\theta$  is the temperature field,  $\tau_0$  is the thermal relaxation time,  $k$  is the thermal conductivity of the material,  $C_v$  is the specific heat constant of the material,  $\mu$  and  $\nu$  are material-specific coefficients that characterise the dependency of the stress on the rate of the deformation gradient and temperature respectively,  $\rho$  is the density of the material,  $\theta_1$  is a positive constant that characterises a critical temperature of the material, and  $k_i$ ,  $i = 1, 2, 3$  are material-specific constants that characterise the material's free energy. The right-hand sides of system (1),  $F$  and  $G$ , represent distributed mechanical and thermal loadings of the body.

Although this model was developed on the mesoscale level, it should be noted that the connection between different levels of descriptions manifests itself in the constitutive theories where one has to couple (a) the free energy, (b) the stress, and (c) the heat flow of the crystal with deformation, temperature and, when necessary, with their temporal and spatial gradients [14]. When only equilibrium properties of the material are of interest, such theories can be simplified with the stress represented by the derivative of the free energy function with respect to deformation. In model (1) we used the phenomenological Landau-Devonshire free energy function and the Cattaneo-Vernotte model for heat conduction. The shear strain on the habit plane (the contact plane between both phases) was taken as the basic deformation variable. In some cases we have to deal with habit planes of discontinuous deformation (for example, considering domain walls between martensitic variants, nucleation phenomena, or studying the interface between martensite and austenite). One way of dealing with such situations is to incorporate the Ginzburg term into the model (modify the Landau-Devonshire free energy function by adding the couple stresses term). Apart from the fact that this approach is disputable [26], it appeared that with reported values of the Ginzburg coefficient ( $10^{-10}$ – $10^{-12}$ ) the gradient strain term has a negligible effect in the class of experiments we performed [14]. As we shall see in Section 5 a similar situation arises when the 3D Landau-type model is reduced to one dimension.

The model (1) was completed by appropriate initial and boundary conditions and was solved with respect to  $(u, \theta)$  in the spatial-temporal region  $Q = \{(x, t) \mid 0 \leq x \leq L, 0 \leq$



$t \leq T_f$ }, where  $L$  is the length of the structure and  $T_f$  is the required time of observation. The initial conditions for the model (1) were taken in the following form

$$u(x, 0) = u^0(x), \quad v(x, 0) = \frac{\partial u}{\partial t}(x, 0) = u^1(x), \quad \theta(x, 0) = \theta^0(x), \quad \frac{\partial \theta}{\partial t}(x, 0) = \theta^1(x), \quad (2)$$

with specified functions  $u^0, u^1, \theta^0, \theta^1$ . Boundary conditions are problem-specific [14]. In our experiments: mechanical boundary conditions were either specified stress or specified displacement,

$$s(0, t) = s_1(t), \quad s(L, t) = s_2(t), \quad \text{or} \quad u(0, t) = u_1(t), \quad u(L, t) = u_2(t); \quad (3)$$

thermal boundary conditions are those of specified heat flux

$$\frac{\partial \theta}{\partial x}(0, t) = \bar{\theta}_1(t), \quad \frac{\partial \theta}{\partial x}(L, t) = \bar{\theta}_2(t), \quad (4)$$

where functions  $s_i(t)$  (or  $u_i(t)$ ) and  $\bar{\theta}_i(t)$ ,  $i = 1, 2$  were given.

In this paper we continue investigation of meso-scale models of the Landau-type with the emphasis on the modelling of the copper-based shape memory alloy copper-aluminium-nickel. Recall that in the parent high temperature phase (austenite) the copper-based SMAs (such as CuZnAl and CuAlNi) has an ordered body-centred cubic (BCC) lattice. In the phase transformation “each” cubic cell of austenite is transformed into a tetragon, forcing the parent phase to be transformed to an ordered and twinned martensite. Therefore, it is fundamental to this type of transformations that both the parent austenitic phase and the martensitic product are ordered. In the general case one has to deal with 24 crystallographically equivalent martensitic variants (due to the transformation from the 48th order cubic symmetry group of the parent phase to the 2nd order monoclinic group of the product phase). The twinning property of the martensite is the result of minimisation of the stress on the habit plane. Therefore, as follows from the Falk deformation theory [6], due to high interface mobilities between martensite variants and between austenite and martensite variants, for the shape memory effect to occur this plane should be invariant. However, on the *micro-deformation level* (where only the lattice deformation, i.e. the Bain strain, is taken into account) the invariant habit plane does not exist [6]. Indeed, in the martensitic phase transformation the atomic displacements are very small and one can assume that no atomic migration is required for this transformation. Atoms cooperatively rearrange to form a new crystal structure. As a result of this assumption on the *mesoscale deformation level* we consider a coupled effect of the Bain strain and the lattice-invariant shearing mechanism. In the copper-based alloys of interest (CuZnAl and CuAlNi) the lattice-invariant strain is realised as a regular twinning on layers resulting from  $\{110\}$ -planes (called twinning or basal planes) of the BCC lattice (every third layer twins to form a large monoclinic martensite unit cell). It is this coupling effect between the Bain strain and the regular twinning that leads to “almost” invariant plane strain, i.e. a stress-free interface between austenite and martensite.

Now, when the habit plane is stress-free the sheared martensitic volume element will not fit into the region it occupied when it was in the austenitic state [6]. However, this

problem is easily solved on the *macroscopic deformation level* where we assume that the martensitic inclusion does not form as a single martensitic variant. A self-accommodating group of martensitic variants is formed into an aggregate of several martensitic variants, the so-called domain (sometimes called a microstructure) [6, 13]. For such domains the average deformation of their components cancel out. Due to this, on cooling the phase transformation from austenite to martensite occurs without a macroscopic shape change (scale of  $10^{-4}$  m or larger) exhibiting a “ferroelastic” type of stress-strain curves. However, when the transformation is induced by a stress, in the temperature range where the stress-free austenite is stable, we have to deal with pseudoelastic stress-strain curves. One of the approaches that allow work on the macroscopic scale (where the deformation defined on a length scale of  $100\text{ }\mu\text{m}$  or more) stems from Frémond’s work (see references in [2]) and is based on the introduction of an internal variable that characterises fractions of austenite and martensite variants in shape memory alloys. We shall not consider this approach in this paper. We only note that one may expect that the Landau theory on the mesoscale level used in this paper is a consequence of the Landau theory on the microscale level and the constitutive relations of the macroscopic theories (including the Frémond theory) have to follow from the Landau theory considered on the mesoscale level. However, the construction of the hierarchy

Microscale Landau theory  $\Rightarrow$  Mesoscale Landau theory  $\Rightarrow$  Macroscopic theories

is just at the beginning of its development [6]. Hereafter we concentrate on a particular Landau-type models developed on the mesoscale level [5].

#### 4 Three-dimensional Falk-Konopka free energy function and a Landau-type model for the dynamics of shape memory alloys

Numerical analysis of Landau-type models for the description of shape-memory-alloy dynamics has been typically restricted to the one-dimensional case [17, 9, 10]. Three-dimensional modelling in this field is traditionally associated with the application of Frémond’s type models [2]. At the time of writing this paper we are not aware of any computational results obtained with the later models for physically realistic data. The Frémond models consider the phase proportions as thermodynamic quantities and typically include strain gradient terms to account for interfacial energies. This leads to a smoothing term in the momentum balance equation and simplifies analytical analysis of the models (see also Section 3). In the terminology discussed in Section 3, Frémond’s models are considered on the macroscopic scale with temperature, macroscopic strain, strain gradient and the volumetric proportions of austenite and martensites (usually restricted by only two variants) being state variables. Such macroscale models ignore the internal atomic and mesoscale structures of a material using the assumption that the phases simultaneously present **at each point** of the material with appropriate proportions. In this case we have to deal with self-accommodating groups of martensite as a result of the deformation of a macroscopic sample, as explained in the previous section. We are

concerned with a smaller scale, which however is larger than the scale of the monoclinic lattice (i.e. the Bain strain is beyond of the resolution of our models). More precisely, our models describe the phase-transition between body-centred cubic austenite and monoclinic martensite variants on the mesoscopic scale. In order to describe the macroscopic behaviour of shape-memory-alloys an additional averaging (over the different martensite variants forming the macroscopic sample) procedure is required (see [5] and references therein).

Mathematical description of the appropriate mesoscale measure starts from the approximation by a polynomial (with coefficients depending on temperature) with respect to an order parameter characterising the phase transformation as follows [5, 14]

$$\Psi(\epsilon, \theta) = \psi^0(\theta) + \sum_{i=1}^{\infty} \psi^i(\epsilon, \theta) \quad (5)$$

where independent material parameters of the  $n$ -th order for  $n = 1, 2, \dots$  are determined through strain invariants,  $\mathcal{I}_j^n$  as follows

$$\psi^n = \sum_{j=1}^{j^n} \psi_j^n \mathcal{I}_j^n \quad \text{and} \quad \psi^0(\theta) = \psi_0^0(\theta). \quad (6)$$

To make the free energy function invariant with respect to the symmetry group of austenite, the upper limit of the sum in (6),  $j^n$ , is chosen as the number of all invariant directions associated with a representation of the 48th order cubic symmetry group of the parent (austenite) phase.

For the copper-based alloys it is possible to reduce the number of required parameters in (5) to only 10 material constants (in the general case, temperature dependent) [5]

$$\Psi = \psi^0(\theta) + \sum_{i=1}^3 \psi_i^2 \mathcal{I}_i^2 + \sum_{i=1}^5 \psi_i^4 \mathcal{I}_i^4 + \sum_{i=1}^2 \psi_i^6 \mathcal{I}_i^6, \quad (7)$$

where the strain invariants  $\mathcal{I}_i^n$  of second, forth and sixth orders of the 48th order cubic symmetry group of the parent phase are determined as follows

$$\begin{aligned} \mathcal{I}_1^2 &= \frac{1}{9}(\text{tr}(\epsilon_{ij}))^2, \quad \mathcal{I}_2^2 = \frac{1}{12}(2\epsilon_{33} - \epsilon_{11} - \epsilon_{22})^2 + \frac{1}{4}(\epsilon_{11} - \epsilon_{22})^2, \\ \mathcal{I}_3^2 &= \epsilon_{23}^2 + \epsilon_{13}^2 + \epsilon_{12}^2, \quad \mathcal{I}_1^4 = (\mathcal{I}_2^2)^2, \quad \mathcal{I}_2^4 = \epsilon_{23}^4 + \epsilon_{13}^4 + \epsilon_{12}^4, \quad \mathcal{I}_1^6 = (\mathcal{I}_2^2)^3 \\ \mathcal{I}_3^4 &= (\mathcal{I}_3^2)^2, \quad \mathcal{I}_4^4 = \mathcal{I}_2^2 \mathcal{I}_3^2, \quad \mathcal{I}_5^4 = \epsilon_{23}^2 \left[ \frac{1}{6}(2\epsilon_{33} - \epsilon_{11} - \epsilon_{22}) - \frac{1}{2}(\epsilon_{11} - \epsilon_{22}) \right]^2 + \\ &\quad \epsilon_{13}^2 \left[ \frac{1}{6}(2\epsilon_{33} - \epsilon_{11} - \epsilon_{22}) + \frac{1}{2}(\epsilon_{11} - \epsilon_{22}) \right]^2 + \frac{1}{9}\epsilon_{12}^2(2\epsilon_{33} - \epsilon_{11} - \epsilon_{22})^2, \\ \mathcal{I}_2^6 &= \frac{1}{36}(2\epsilon_{33} - \epsilon_{11} - \epsilon_{22})^2 \left( \frac{1}{36}(2\epsilon_{33} - \epsilon_{11} - \epsilon_{22})^2 - \frac{1}{4}(\epsilon_{11} - \epsilon_{22})^2 \right)^2. \end{aligned} \quad (8)$$

Due to the symmetry, the strain tensor  $\epsilon_{ij}$ ,  $i, j = 1, 2, 3$  forms a 6 dimensional space with the basis  $\phi_K$ ,  $K = 1, \dots, 6$  [11]

$$\boldsymbol{\epsilon} = \sum_{K=1}^6 \epsilon_K \phi_K, \quad (9)$$

where

$$\epsilon_1 = \epsilon_{11}, \quad \epsilon_2 = \epsilon_{22}, \quad \epsilon_3 = \epsilon_{33}, \quad \epsilon_4 = 2\epsilon_{23}, \quad \epsilon_5 = 2\epsilon_{13}, \quad \epsilon_6 = 2\epsilon_{12}. \quad (10)$$

We assume that the strain tensor is coupled to the spatial displacements  $\mathbf{u} = (u_1, u_2, u_3)$  of the material point with Lagrangian coordinates  $\mathbf{x} = (x_1, x_2, x_3)$  at time  $t$  by the Cauchy relation

$$\epsilon_{ij}(\mathbf{x}, t) = \frac{1}{2} \left[ \frac{\partial u_i(\mathbf{x}, t)}{\partial x_j} + \frac{\partial u_j(\mathbf{x}, t)}{\partial x_i} \right], \quad i, j = 1, 2, 3. \quad (11)$$

Finally, to complete the definition of the free energy function (7) we specify the parameters  $\psi_i^j$  ( $j = 0, i = 0$ ;  $j = 2, i = 1, 2, 3$ ;  $j = 4, i = 1, \dots, 5$ ;  $j = 6, i = 1, 2$ ) which for the copper-aluminium-nickel alloys (Cu is 14 wt% and Al is 3 wt%) are

$$\begin{aligned} \psi_1^2 &= 5.92 \times 10^6 \text{ g}/(\text{ms}^2\text{cm}), \quad \psi_2^2 = (1.41 \times 10^5 + 46(\theta - 300)) \text{ g}/(\text{ms}^2\text{cm}), \\ \psi_3^2 &= (1.48 \times 10^6 + 940(\theta - 300)) \text{ g}/(\text{ms}^2\text{cm}), \quad \psi^0 = -\alpha_1 \theta \ln[(\theta - \theta_0)/\theta_0] \text{ g}/(\text{ms}^2\text{cm}), \\ \psi_1^4 &= (-1.182 \times 10^8 + 3.55 \times 10^5(\theta - 300)) \text{ g}/(\text{ms}^2\text{cm}), \\ \psi_2^4 &= 3.13 \times 10^9 \text{ g}/(\text{ms}^2\text{cm}), \quad \psi_3^4 = 1.64 \times 10^9 \text{ g}/(\text{ms}^2\text{cm}), \\ \psi_4^4 &= -5.53 \times 10^8 \text{ g}/(\text{ms}^2\text{cm}), \quad \psi_5^4 = -4.27 \times 10^8 \text{ g}/(\text{ms}^2\text{cm}), \\ \psi_1^6 &= 3.35 \times 10^{10} \text{ g}/(\text{ms}^2\text{cm}), \quad \psi_2^6 = 3.71 \times 10^{11} \text{ g}/(\text{ms}^2\text{cm}), \end{aligned} \quad (12)$$

where  $\alpha_1$  is the heat capacity of the material.

Having the free energy function, we define the shear stress by its three components: the quasi-conservative component,  $\mathbf{s}^q$ , the stress component due to mechanical dissipation,  $\mathbf{s}^m$ , and the stress component due to thermal dissipations,  $\mathbf{s}^t$ , (the latter is assumed to be negligible),

$$\mathbf{s} = \mathbf{s}^q + \mathbf{s}^m + \mathbf{s}^t, \quad \text{with} \quad \mathbf{s}^q = \rho \frac{\partial \Psi}{\partial \boldsymbol{\epsilon}}, \quad \mathbf{s}^m = \rho \mu \frac{\partial \boldsymbol{\epsilon}}{\partial t}, \quad \mathbf{s}^t = \mathbf{0}. \quad (13)$$

If we assume that  $\mu = 0$ , then the relationship  $\mathbf{s} = \mathbf{0}$  (i.e. the derivative of the free energy function with respect to  $\boldsymbol{\epsilon}$ ) gives the necessary conditions for the minima of  $\Psi$ . Although we have 6 such conditions (see the representation (9)), we are only interested in the conditions associated with austenite and martensite phases. The first such conditions,

$\epsilon = \mathbf{0}$ , is associated with the austenite phase which is stable when the Hessian of  $\Psi$  (computed with respect to  $\epsilon$ ) is positive definite. The second condition, derived in [5],

$$\epsilon = \begin{pmatrix} 2\alpha & \beta & 0 \\ \beta & 0 & -\beta \\ 0 & -\beta & -2\alpha \end{pmatrix} \quad (14)$$

corresponds to a monoclinic spontaneous strain with temperature-dependent parameters  $\alpha$  and  $\beta$  subject to the following system of equations [5]

$$\begin{cases} 48\alpha^4\psi_1^6 + 8\alpha^2\psi_1^4 + 2\beta(\psi_4^4 + \psi_5^4) + \psi_2^2 = 0, \\ 4\alpha^2(\psi_4^4 + \psi_5^4) + 2\beta^2(\psi_2^4 + 2\psi_3^4) + \psi_3^2 = 0. \end{cases} \quad (15)$$

Given  $\alpha^2$ , from (15) we deduce  $\beta^2$  and then the magnitude of the shear strain vector by the formula [5]

$$|\epsilon|^2 = 2 \left[ 1 - \sqrt{1 - 8(2\alpha^2 + \beta^2)} \right]. \quad (16)$$

The strain invariants in this situation are

$$\begin{aligned} \mathcal{I}_1^2 = 0, \quad \mathcal{I}_2^2 = 4\alpha^2, \quad \mathcal{I}_3^2 = 2\beta^2, \quad \mathcal{I}_1^4 = 16\alpha^4, \quad \mathcal{I}_2^4 = 2\beta^4, \\ \mathcal{I}_3^4 = 4\beta^4, \quad \mathcal{I}_4^4 = 8\alpha^2\beta^2, \quad \mathcal{I}_5^4 = 8\alpha^2\beta^2, \quad \mathcal{I}_1^6 = 64\alpha^6, \quad \mathcal{I}_2^6 = 0. \end{aligned} \quad (17)$$

For the given temperature these relations allow us to define the stress and the free energy function as functions of the monoclinic spontaneous strain defined by the matrix (14).

Now we are in the position to describe the dynamics of shape-memory alloys in the 3D case by the coupled system that consists of the equation of motion and the energy balance equation

$$\begin{cases} \rho \frac{\partial^2 \mathbf{u}}{\partial t^2} = \nabla_{\mathbf{x}} \cdot \mathbf{s} + \mathbf{F}, \\ \rho \frac{\partial e}{\partial t} - \mathbf{s}^T : (\nabla \mathbf{v}) + \nabla \cdot \mathbf{q} = g, \end{cases} \quad (18)$$

where  $\mathbf{F}$  and  $g$  are given distributed mechanical and thermal loadings of the body and  $\mathbf{a}^T : \mathbf{b} = \sum_{i,j=1}^3 a_{ij}b_{ij}$  is the standard notation for the rank 2 tensors  $\mathbf{a}$  and  $\mathbf{b}$ . The velocity function  $\mathbf{v}$ , the internal energy function  $e$  and the heat flux  $\mathbf{q}$  are defined as follows

$$\mathbf{v} = \frac{\partial \mathbf{u}}{\partial t}, \quad e = \Psi - \theta \frac{\partial \Psi}{\partial \theta}, \quad \mathbf{q} = -k \nabla \theta - \alpha \frac{\partial k \nabla \theta}{\partial t}, \quad (19)$$

where the last expression is an approximation to the solution of the 3D Cattaneo-Vernotte equation [14] (computational experiments were performed with the classical Fourier law where  $\alpha = 0$ ).

The embedding of constitutive equations that couples the free energy, the stress and the heat flow with the state variables into the basic laws of mechanics (18) provides the

foundation for the mathematical modelling of shape-memory-alloy dynamics. Of course, the specification of constitutive equations for shape memory materials is far from being unique and the development of thermodynamic constitutive models for these materials is an active area of research [4, 1, 8, 12]. Recently, Lurier [12] proposed a quite general approach to the construction of constitutive models for shape memory alloys (a number of earlier developed structural-analytical, phenomenological and micromechanical models follow from his model as special cases). Although we do not consider these constitutive models here, in the next section we develop a computer-algebra-based technique which, with appropriate modifications, is capable of effectively incorporating those models.

## 5 The construction of low-dimensional slow manifold models for the dynamics of shape memory alloys

We consider a shape memory alloy slab which is very large in the  $x = x_1$  direction compared to its thickness of  $2b$  in the  $y = x_2$  direction ( $-b < y < b$ ) and neglect any motion and dependence in the  $x_3$  direction. In this section, we reduce the 3D model for the dynamics of shape-memory-alloys described in Section 4 to a simpler model expressed in terms of the amplitudes of cross-sectional averages of critical quantities. The basic idea of our approach is to express the physical fields in terms of asymptotic sums in these amplitudes and their longitudinal gradients. The asymptotic approximation is found to solve the system (18) describing the dynamics of SMA. This technique is at the heart of centre manifold theory, originated by Pliss [18]. During the last decade this technique has been successfully linked to computer algebra approaches and apply to a number of problems in continuum mechanics [3, 20, e.g.]. It is this linkage that makes the centre manifold method a powerful tool in the analysis of complex mathematical models. We refer the reader to [23, 7] (and the references therein) for the rigorous analysis of the reduction procedure of a system onto a centre manifold. Here, using similar techniques, we develop the slow, sub-centre manifold [24, §7] model by adapting the analysis of beam theory developed by [19] to the nonlinear dynamics of SMA. We show, using the computer algebra package REDUCE, how to derive systematically (up to the arbitrary order of accuracy) an accurate low-dimensional model for the description of thermomechanical behaviour of thin slabs in shape memory alloy materials.

For the unforced dynamics ( $\mathbf{F} = \mathbf{0}$ ,  $g = 0$ ) we derive a model that describes the dynamics of slowly-varying (along the slab) modes. We note that in the presence of a time-dependent forcing, the system may substantially deviate from the slow manifold and the use of geometric projection of initial conditions is required to determine the forcing appropriate for the model. As for the boundary conditions, theory typically employs arguments based upon the spatial evolution away from the boundary which are applied to the original model and its approximation (see [20] and references therein). Here, we use “zero-stress” & “thermal-insulation” boundary conditions specified on  $y = \pm b$ , and “pinned” & “insulating ends” boundary conditions provide a leading approximation in the “long” direction (this, however, requires a quite delicate analysis which is outside the scope of this paper

[20]).

We model the long-wavelength, small-wavenumber modes along the slab. For simplicity in this first approach, we also assume that the effect of dissipation processes is negligible (we set  $\alpha = \mu = 0$ ). Then, the eigenvalue analysis of the cross-slab modes shows that generally there is a zero eigenvalue of multiplicity five which corresponds to large-scale longitudinal waves, large-scale bending, and one heat mode (since dissipation effects were neglected, all other eigenvalues are pure imaginary). Thus there exists a slow sub-centre manifold based upon these five modes. This fact allows us to construct a new model on the sub-centre manifold (although the model will not have an assured guarantee of asymptotic completeness [23, 7, 3]).

Since the leading order structure of the critical eigenmodes are constant across the slab, the amplitudes of the critical modes are chosen to be the cross-sectional averages

$$U_i(x, t) = \overline{u_i}, \quad V_i(x, t) = \overline{v_i}, \quad \Theta'(x, t) = \overline{\theta'}, \quad (20)$$

where an overbar denotes the  $y$ -average quantity and  $\theta' = \theta - \theta_0$  ( $\theta_0 = 300^\circ K$ ). Our low-dimensional model is written in terms of these parameters. We seek the low-dimensional invariant manifold upon which these amplitudes evolve slowly:

$$u_i = \mathcal{U}_i(\mathbf{U}, \mathbf{V}, \Theta'), \quad v_i = \mathcal{V}_i(\mathbf{U}, \mathbf{V}, \Theta'), \quad i = 1, 2, \quad \theta = \mathcal{T}(\mathbf{U}, \mathbf{V}, \Theta'), \quad (21)$$

$$\text{where} \quad \frac{\partial U_i}{\partial t} = V_i, \quad \frac{\partial V_i}{\partial t} = g_i(\mathbf{U}, \mathbf{V}, \Theta'), \quad \frac{\partial \Theta'}{\partial t} = g_\theta(\mathbf{U}, \mathbf{V}, \Theta'). \quad (22)$$

The expressions (21) are substituted into the model (18) and the resulting system is solved to some order in the small parameters  $\partial_x$ ,  $E = \|\mathbf{U}_x\| + \|\mathbf{V}_x\|$  and  $\vartheta = \|\Theta'\|$  with the computer algebra package REDUCE. Thus, here we treat the strains as small, as measured by  $E$ , while permitting asymptotically large displacements and velocities.

We use  $\mathcal{O}(E^p + \partial_x^q + \vartheta^r)$  to denote an error in the model obtained by neglecting all terms involving  $\partial_x^{\beta_1} E^{\beta_2} \vartheta^{\beta_3}$  such that  $\beta_1/p + \beta_2/q + \beta_3/r \geq 1$ . Then with errors  $\mathcal{O}(E^5 + \partial_x^{5/2} + \vartheta^{5/2})$  the displacement and temperature fields of the slow manifold, in terms of the amplitudes and the scaled transverse coordinate  $Y = y/b$ , are

$$u_1 \approx U_1 - YbU_{2x} + 0.15(3Y^2 - 1)b^2U_{1xx}, \quad (23)$$

$$u_2 \approx U_2 - (0.9 - 3.05e-5\Theta')YbU_{1x} + 0.15(3Y^2 - 1)b^2U_{2xx} \\ - 141YbU_{1x}^3 + 1.00e-4(3Y - Y^3)b^3V_{1x}^2U_{1x}, \quad (24)$$

$$\theta \approx 300 + \Theta' - 2.43e6(3Y - Y^3)b^3(V_{1x}U_{2xx} + U_{1x}V_{2xx}) \\ - 25.1(7 - 30Y^2 + 15Y^4)V_{1x}^3U_{1x}. \quad (25)$$

As we noted in [14], the mechanical and thermal field approximations represented by (23)–(25) have cross-slab structure. In particular, the sideways deformation  $u_2$  (which is a nonlinear function of the longitudinal strains) of the shape memory alloy feed back at higher order to contribute to and complicate the longitudinal and thermal dynamics.

The computer algebra code to derive these expressions is available upon request to the authors. Finally, with errors  $\mathcal{O}(E^8 + \partial_x^4 + \vartheta^4)$  the model for the longitudinal dynamics on this slow manifold is

$$\left. \begin{aligned} \rho \frac{\partial V_1}{\partial t} &= c_1 U_{1xx} + \gamma_1 b^2 U_{1xxxx} \\ &\quad + \partial_x \left[ (c_2 \Theta' - c_3 \Theta'^2) U_{1x} - (c_4 - c_5 \Theta') U_{1x}^3 + c_6 U_{1x}^5 \right. \\ &\quad \left. + (c_7 - c_8 \Theta') b^2 V_{1x}^2 U_{1x} + c_9 b^4 V_{1x}^4 U_{1x} - c_{10} b^2 V_{1x}^2 U_{1x}^3 \right], \\ \rho \frac{\partial V_2}{\partial t} &= -\gamma_2 b^2 U_{2xxxx}, \\ C_v \frac{\partial \Theta'}{\partial t} &= \kappa \Theta'_{xx} + (c_{11} + c_{12} \Theta' - c_{13} \Theta'^2) U_{1x} V_{1x} \\ &\quad + (c_{14} + c_{15} \Theta') V_{1x} U_{1x}^3 + c_{18} V_{1x} U_{1x}^5 \\ &\quad - (c_{16} + c_{17} \Theta') b^2 V_{1x}^3 U_{1x} - c_{19} b^2 V_{1x}^3 U_{1x}^3 - c_{20} b^4 V_{1x}^5 U_{1x} \\ &\quad + c_{21} b^2 U_{1xx} V_{1xx} + c_{22} b^2 U_{2xx} V_{2xx} + \partial_x^2 [-c_{23} b^2 U_{1x} V_{1x}], \\ \frac{\partial U_i}{\partial t} &= V_i, i = 1, 2, \end{aligned} \right\} \quad (26)$$

where coefficients  $c_k$ ,  $k = 1, \dots, 23$ , are positive material constants.

In the first equation of this system the first line in the right-hand side describes linear dispersive elastic waves along the slab, whereas the second line gives the temperature dependent quintic stress-strain relation of the shape memory alloy (the analogue of the classical Falk representation). The remaining terms describe the effects due to rates of change of the strain [14]. The first two lines in the right-hand side of the third equation of the system describes the diffusion of heat generated/absorbed by mechanical strains,  $\Theta U_{1x}^p V_{1x}$  terms. The remaining lines shows the effects of the internal pattern of mesoscopic strain. Finally, note that since there is no coupling of the longitudinal dynamics to the bending modes of the slab (to this order of truncation), the second equation of the system is the classic beam equation.

## 6 Numerical examples

Computational experiments reported in this section were performed for a thin single-crystal CuAlNi slab. The thermomechanical parameters for this material were chosen to be (see Section 2)

$$\rho = 7.12 \text{ g/cm}^3, \quad k = 0.0030 \text{ cmg}/(\text{ms}^3\text{K}), \quad C_v = \rho \alpha_1 = 26.6 \text{ g}/(\text{ms}^2\text{cmK}). \quad (27)$$

By assuming the slab is thin enough so that in effect  $b = 0$  we reduce our model (26) to



the following differential algebraic system

$$\left. \begin{aligned} \rho \frac{\partial V_1}{\partial t} &= \frac{\partial s}{\partial x} + F, \\ C_v \frac{\partial \Theta'}{\partial t} &= k \frac{\partial^2 \Theta'}{\partial x^2} + (c_{11} + c_{12} \Theta' - c_{13} (\Theta')^2) \frac{\partial U_1}{\partial x} \frac{\partial V_1}{\partial x} + \\ &\quad + (c_{14} + c_{15} \theta') \frac{\partial V_1}{\partial x} \left( \frac{\partial U_1}{\partial x} \right)^3 + c_{18} \frac{\partial V_1}{\partial x} \left( \frac{\partial U_1}{\partial x} \right)^5 + g, \\ s &= (c_1 + c_2 \theta' - c_3 (\theta')^2) \frac{\partial U_1}{\partial x} - (c_4 - c_5 \theta') \left( \frac{\partial U_1}{\partial x} \right)^3 + c_6 \left( \frac{\partial U_1}{\partial x} \right)^5, \\ \frac{\partial U_1}{\partial t} &= V_1. \end{aligned} \right\} \quad (28)$$

This system is then discretised in space using second-order approximations in space on staggered grids and solved with the differential-algebraic solver described in our earlier papers [14, 15]. The coefficients in the model (28) are obtained directly from the model (26) and for CuAlNi alloys have the following numerical values

$$\begin{aligned} c_1 &= 1.91 \times 10^6, & c_2 &= 592, & c_3 &= 0.00931, & c_4 &= 2.75 \times 10^9, & c_5 &= 8.42 \times 10^6, \\ c_6 &= 4.56 \times 10^{11}, & c_{11} &= 1.78 \times 10^5, & c_{12} &= 586, & c_{13} &= 5.94, \\ c_{14} &= 2.53 \times 10^9, & c_{15} &= 8.11 \times 10^6, & c_{18} &= 1.08 \times 10^{12}, & \gamma_1 &= 5.15 \times 10^5. \end{aligned} \quad (29)$$

If the thickness of the slab is not negligible compared to its length (taken to be 1 cm in our experiments), then the inclusion of all “ $b$ ”-dependent terms in the model (28) is required. The corresponding coefficients for CuAlNi have the following values

$$\begin{aligned} c_7 &= 1811, & c_8 &= 5.64, & c_9 &= 0.728, & c_{10} &= 2.51 \times 10^3, & \gamma_2 &= 6.36 \times 10^5 \\ c_{16} &= 36.8, & c_{17} &= 0.00761, & c_{18} &= 1.08 \times 10^{12}, & c_{19} &= 1.016 \times 10^6, \\ c_{20} &= 0.0116, & c_{21} &= 1.05 \times 10^4, & c_{22} &= 5.92 \times 10^4, & c_{23} &= 5228. \end{aligned} \quad (30)$$

In the first experiment we study the dynamics of a shape memory alloy sample under the uniform mechanical forcing  $F = -1 \times 10^{-3} \text{ g}/(\mu\text{s}^2\text{cm}^2)$  and time-dependent distributed heating/cooling according to the rule  $g = 1.15 \times 10^{-3} \pi \sin^3(t\pi/15) \text{ g}/(\mu\text{s}^3\text{cm})$ . The initial displacement field was taken to be

$$u^0(x) = \begin{cases} 0.0636 x, & 0 \leq x \leq 1/2, \\ 0.0636 (1 - x), & 1/2 \leq x \leq 1. \end{cases} \quad (31)$$

We used “pinned ends” and “thermal insulation” boundary conditions. With the initial temperature  $350^\circ\text{K}$  the dynamics of the sample on the time interval  $0 \leq t \leq 30 \mu\text{s}$  is presented in Figure 1. Upon heating, the martensite phase becomes metastable. Under appropriate thermomechanical conditions, this metastability may lead to the transformation of martensite phase into austenite. An attempt of this transformation is accompanied by a certain decrease in temperature, clearly visible in Figure 1. This decrease compensates for the given thermal forcing and the resulting temperature is insufficient to

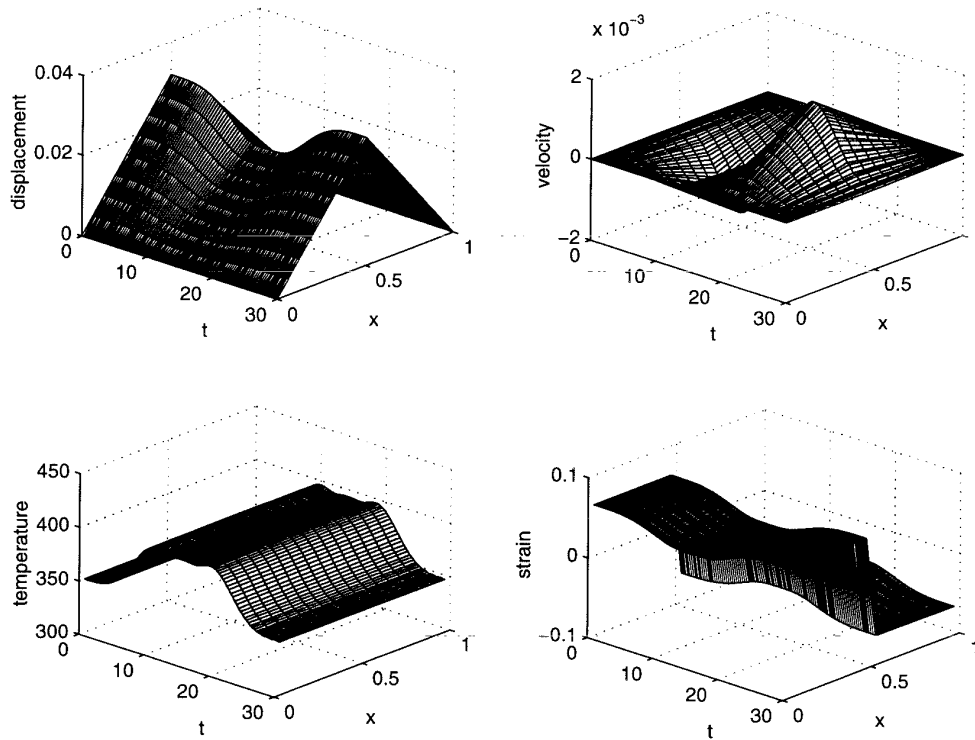


Figure 1: Thermal forcing of a CuAlNi rod.

transform martensite into austenite on this scale of observation. Therefore, upon cooling, the martensite phase returns to its original stable state.

The second experiment uses a purely mechanical ( $g = 0$ ) time-dependent forcing given by the formula  $F = 0.03 \sin^3(\pi t/15) \text{ g}/(\text{cm}^2 \mu\text{s}^2)$ . We use the same boundary conditions as before. Starting with the initial configuration  $u^0 = 0$  at the temperature  $350^\circ\text{K}$  we observe a strong coupling phenomenon between thermal and mechanical fields (see Figure 2). This phenomenon reminds us of the result of Experiment 2 from [14], where the dynamics of AuCuZn alloys was investigated. It is evident that it is much more difficult to retain the austenite phase in copper-aluminium-nickel compared to AuCuZn alloys and the computational analysis of stability of the parent phase for CuAlNi requires further investigation.

## 7 Conclusions

In this paper we presented results of an investigation into the thermomechanical behaviour of a copper-aluminium-nickel shape memory alloy. Using the three dimensional Landau theory describing the martensitic phase transformation of shape memory alloys we developed a systematic approach to the shape memory alloy modelling based on centre manifold techniques implemented in computer algebra packages. In particular, we

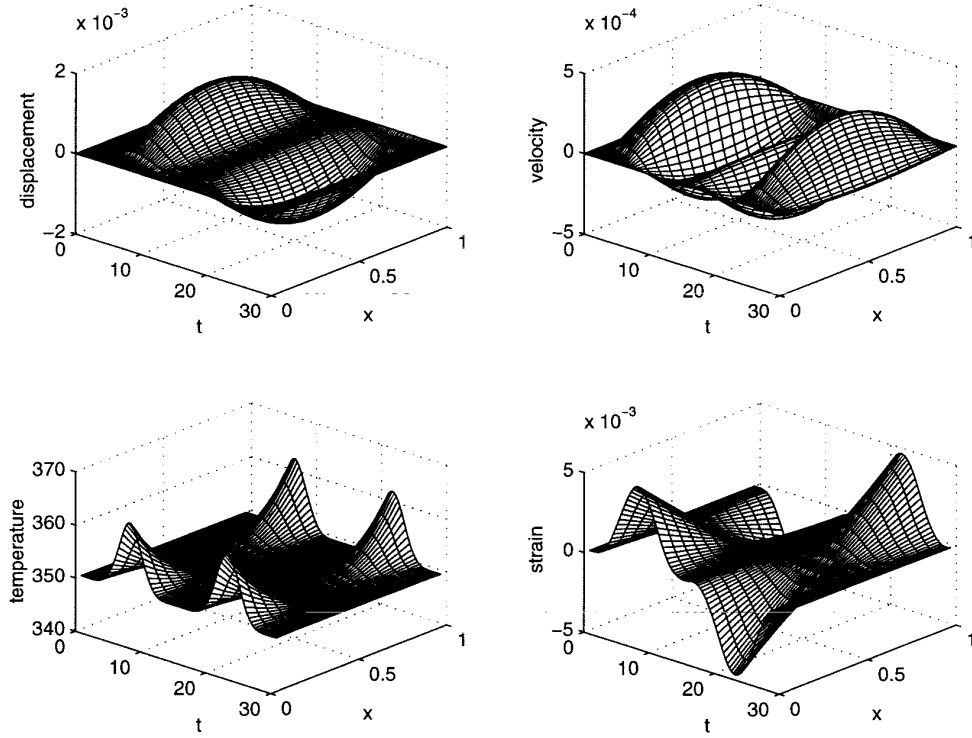


Figure 2: Mechanical forcing of a CuAlNi rod.

constructed a new model for the description of the shape memory alloy dynamics that allows us to describe essential dynamic behaviour of the system by determining the evolution on the crucial subset of all possible modes. The numerical scheme based on an effective differential-algebraic integrator provides a robust approach to the analysis of shape memory alloy dynamics. This analysis has been used in computational studies of thermomechanical behaviour of CuAlNi alloys.

The implementations of computational results into engineering applications are impeded by the absence of a theory that would allow us to compute thermomechanical characteristics of polycrystallines using such characteristics for single crystal. Effective averaging procedures over the grains are required in order to transfer highly nonlinear stress-strain curves for single crystals to polycrystals [6, 13]. Using such procedures, the technique proposed in our paper can be effectively adapted to the analysis of shape-memory alloy dynamics in polycrystalline structures as well as to other problems on structural phase transitions.

## References

- [1] J.G. Boyd and D.C. Lagudas: *A thermodynamic constitutive model for shape memory materials, Part 1*. Int. J. Plasticity, **12**, No. 6, 805, (1996).

- [2] P. Colli and J. Sprekels: *Global Existence for a Three-Dimensional Model for the Thermo-Mechanical Evolution of Shape Memory Alloys*. Nonlinear Analysis: TMA, **18**, 873 – 888, (1992).
- [3] S.M. Cox and A.J. Roberts: *Centre manifolds of forced dynamical systems*. J. Austral. Math. Soc. Ser. B, **32**, 401–436, (1991).
- [4] V.G. DeGiorgi and H. Saleem: *A comparison of a few shape memory alloy constitutive models*. In: V.V. Varadan (ed.), Mathematics and Control in Smart Structures, Proc. of SPIE Vol. 3667, (1999).
- [5] F. Falk and P. Konopka: *Three-dimensional Landau theory describing the martensitic phase transformation of shape-memory-alloys*. J. Phys.: Condens. Matter, **2**, 61–77, (1990).
- [6] F. Falk: *On constitutive theories of shape memory alloys undergoing a structural phase transformation*. Material Science Forum, **123-125**, 91–100, (1993).
- [7] Th. Gallay: *A center-stable manifold theorem for differential equations in Banach spaces*. Commun. Math. Phys., **152**, 249–268, (1993).
- [8] E.J. Graesser, and F.A. Cozzarelli: *A proposed three-dimensional constitutive model for shape memory alloys*. Journal of Intelligent Material Systems and Structures, **5**, 78 – 89, (1994).
- [9] K.-H. Hoffmann and J. Zou: *Finite Element Approximations of Landau-Ginsburg's Equation Model for Structural Phase Transitions in Shape Memory Alloys*. M<sup>2</sup>AN, **29**, 629–655, (1995).
- [10] O. Klein: *Stability and uniqueness results for a numerical approximation of the thermomechanical phase transitions in SMA*. Advances in Mathematical Sciences and Applications (Tokyo), **5**, No. 1, 91 – 116, (1995).
- [11] P. Konopka and F. Falk: *Three-Dimensional Landau Theory Describing the Martensitic Phase Transformation of Shape-Memory Alloys*. Materials Science Forum, **123-125**, 113 – 122, (1993).
- [12] S.A. Lurier: *On thermodynamical constitutive relations for shape memory materials*. Mechanics of Solids, **No. 5**, 110–122, (1997).
- [13] M. Luskin: *On the computation of crystalline microstructure*. Acta Numerica, **5**, 191–257, (1996).
- [14] R.V.N. Melnik and A.J. Roberts: *Approximate Models of Dynamic Thermoviscoelasticity Describing Shape-Memory-Alloy Phase Transitions*. to appear in the Proceedings of the NEMACOM'98, Centre for Mathematics and its Applications, Australian National University, (1999).
- [15] R.V.N. Melnik, A.J. Roberts and K.A. Thomas: *Modelling dynamics of shape-memory-alloys via computer algebra*. In: V.V. Varadan (ed.), Mathematics and Control in Smart Structures, Proc. of SPIE Vol. 3667, (1999).
- [16] N.B. Morgan and C.M. Friend: *Market Strategies for the Commercial Exploitation of Shape Memory Alloys*. J. Phys. IV France (Colloque C5), **7**, 615 – 620, (1997).

- [17] M. Niezgodka and J. Sprekels: *Convergent Numerical Approximations of the Thermomechanical Phase Transitions in Shape Memory Alloys.*, Numer. Math., **58**, 759–778, (1991).
- [18] V.A. Pliss: *A reduction principle in the theory of stability of motion.* Izv. Akad. Nauk. SSSR Ser. Mat., **28**, 1297–1324, (1964).
- [19] A.J. Roberts. *The invariant manifold of beam deformations. Part 1: the simple circular rod.* J. Elas., **30**, 1–54, (1993).
- [20] A.J. Roberts: *Low-dimensional modelling of dynamics via computer algebra.* Comput. Phys. Comm., **100**, 215–230, (1997).
- [21] E. Runtsch: *Shape memory actuators in circuit breakers.* In: T.W. Duering (ed.), Engineering Aspects of Shape Memory Alloys, Butterworth-Heinemann (1990), 330–337.
- [22] L. McDonald Schetky: *Shape memory alloy applications in space systems.* In: T.W. Duering (ed.), Engineering Aspects of Shape Memory Alloys, Butterworth-Heinemann (1990), 170–177.
- [23] L. P. Shilnikov et al: *Canter Manifold. Local Case.* In: L. P. Shilnikov et al, Methods of Qualitative Theory in Nonlinear Dynamics. Part 1, World Scientific (1990), 269–323.
- [24] J. Sijbrand. *Properties of centre manifolds.* Trans. Amer. Math. Soc., **289**, 431–469, (1985).
- [25] W.B. Spillman, J.S. Sirkis and P.T. Gardiner: *Smart materials and structures: what are they?* Smart Mater. Struct., **5**, 247–254, (1996).
- [26] J. Sprekels: *Shape memory alloys: mathematical models for a class of first order solid-solid phase transitions in metals.* Control and Cybernetics, **19**, No. 3-4, 287 – 308, (1990).
- [27] T. Takagi: *Recent research on Intelligent Materials.* Journal of Intelligent Material Systems and Structures, **7**, 346 – 352, (1996).
- [28] J. Van Humbeeck: *Shape Memory Materials: State of the Art and Requirements for Future Applications.*, J. Phys. IV France (Colloque C5), **7**, 3 – 12, (1997).
- [29] M. H. Wu: *Cu-based shape memory alloys.* In: T.W. Duering (ed.), Engineering Aspects of Shape Memory Alloys, Butterworth-Heinemann (1990), 69–88.

# ECCM '99 – TABLE OF CONTENTS

(Note: Number refers to pdf-document on the CD-ROM in folder “Reader”)

## Solid Mechanics

### Material Modelling

<b>O. Allix, J.-F. Deü, P. Ladevèze:</b> <i>A delay-damage-meso-model for the prediction of localization and fracture of laminates subjected to high rate loading</i> .....	<b>552</b>
<b>M. Brünig:</b> <i>Finite element analysis and localization behaviour of elastic-viscoplastic hydrostatic stress-sensitive metals</i> .....	<b>563</b>
<b>J. Chambert, P. Bressolette, A. Vergne:</b> <i>Numerical analyses of void growth and coalescence in work-hardening porous ductile materials</i> .....	<b>570</b>
<b>A. Constantinescu, J. Kichenin:</b> <i>A residual stress analysis involving matter deposit and removal</i> .....	<b>241</b>
<b>R. Denzer, M. Maier:</b> <i>Numerical simulation of the micromechanical energy absorbing mechanisms of aluminium foams</i> .....	<b>579</b>
<b>A. Dorfmann, S. L. Burtcher:</b> <i>A micromechanical elasto-plastic stress-strain model with grain boundary sliding</i> .....	<b>437</b>
<b>J. Ebers-Ernst, D. Dinkler:</b> <i>Modelling of stress-strain behaviour of municipal solid waste</i> .....	<b>255</b>
<b>P. Ladevèze, D. Dureisseix, O. Loiseau:</b> <i>A two-scale computational approach suitable for parallel computing</i> .....	<b>591</b>
<b>T. Lodygowski, E. Oleszkiewicz:</b> <i>Metal-matrix composites under static, dynamic and thermal loading</i> .....	<b>728</b>
<b>J. C. Michel, H. Moulinec, P. Suquet:</b> <i>Effective properties of power-law cell materials</i> .....	<b>656</b>
<b>V. P. Panoskaltsis, K.-D. Papoulia, J. Lubliner, S. Bahuguna:</b> <i>Finite element analysis of rate dependence and failure of concrete</i> .....	<b>347</b>
<b>R. H. J. Peerlings, W. A. M. Brekelmans, R. de Borst, M. G. D. Geers:</b> <i>Gradient-enhanced damage modelling of fatigue failure</i> .....	<b>640</b>
<b>T. Sadowski, S. Samborski:</b> <i>Micromechanical modelling of polycrystalline porous ceramics materials under compressive loading</i> .....	<b>648</b>
<b>S. M. Schlögl, E. van der Giessen:</b> <i>Micromechanics of high temperature hydrogen attack</i> .....	<b>658</b>
<b>A. J. Urbanowski:</b> <i>Unified, finite element based approach to the problem of homogenisation of structural members with periodic microstructure</i> .....	<b>395</b>

<i>structures</i> .....	619
<b>R. V. N. Melnik, A. J. Roberts, K. A. Thomas:</b> <i>Dynamics of shape-memory-alloys: A reduction procedure for 3D models</i> .....	328
<b>A. Suleman, P. A. Moniz, A. P. Costa:</b> <i>Modeling of adaptive composite structures and application to aircraft structures</i> .....	171
<b>H. S. Tzou, R. Ye, H. Bahrami:</b> <i>Multi-DOF actuation and control of wing panels and precision manipulators</i> .....	657

## Concrete

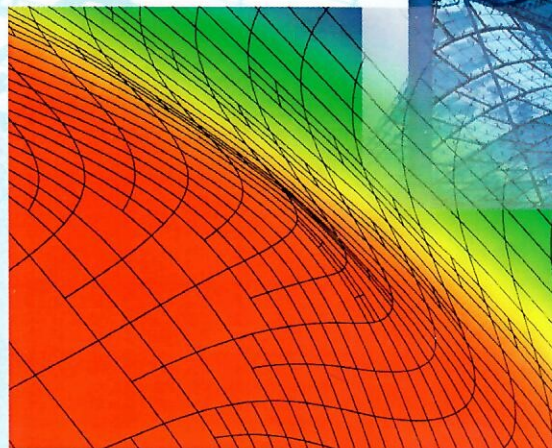
<b>J. Alfaiate, J. R. de Almeida:</b> <i>The study of confined masonry walls submitted to imposed displacements and temperature effects</i> .....	205
<b>P. Dechent, A. Solar, R. Huenchullán, M. Fuentes:</b> <i>Non linear analysis or reinforced concrete walls</i> .....	711
<b>C.-A. Graubner, M. Six:</b> <i>Consistent safety format for non-linear analysis of concrete structures</i> .....	488
<b>G. Horrigmoe:</b> <i>Computer modelling of damaged and repaired concrete structures</i> ...	284
<b>W. Kaufmann:</b> <i>Constitutive modelling of structural concrete subjected to in-plane forces: Cracked membrane model</i> .....	293
<b>R. Meiswinkel, H. Rahm:</b> <i>Modelling tension stiffening in RC structures regarding nonlinear design analysis</i> .....	487
<b>J. Pravida, W. Wunderlich:</b> <i>A plasticity based model and an adaptive algorithm for finite element analysis of reinforced concrete panels in a state of plane stress</i> .....	354
<b>E. J. Sapountzakis, J. T. Katsikadelis:</b> <i>Creep and shrinkage effect on the dynamic analysis of reinforced concrete slab-and-beam structures</i> .....	370
<b>D. Tikhomirov, E. Stein:</b> <i>Anisotropic damage – plastic modelling of reinforced concrete</i> .....	391
<b>G. P. A. G. van Zijl, R. de Borst, J. G. Rots:</b> <i>Finite element analysis of moisture migration, creep, shrinkage and cracking</i> .....	398
<b>H. Walter, L. Baillet, M. Brunet:</b> <i>2D and 3D finite element modelling of anchors in concrete structures</i> .....	402
<b>K. W. Wong, R. F. Warner:</b> <i>Non-linear design of reinforced concrete structures: Safety considerations</i> .....	412

## Concrete Structures

<b>M. Cervera, J. Oliver, T. Prato:</b> <i>Thermo-mechanical analysis of the construction process of roller compacted concrete dams</i> .....	568
---	-----



Solids,  
Structures, and  
Coupled Problems  
in Engineering



Proceedings of the  
**European Conference  
on Computational  
Mechanics 1999**  
Editor: W. Wunderlich

# ECCM '99

European Conference on Computational Mechanics

August 31 – September 3, 1999, Munich, Germany

